

PHYSICAL REVIEW B

CONDENSED MATTER

THIRD SERIES, VOLUME 45, NUMBER 1

1 JANUARY 1992-I

Low-temperature structural phase transitions in $\text{NH}_4L(\text{SO}_4)_2 \cdot 4\text{H}_2\text{O}$ ($L = \text{La} - \text{Dy}$): Specific-heat measurements

S. Jasty and V. M. Malhotra

*Department of Physics and Molecular Science Program, Southern Illinois University at Carbondale,
Carbondale, Illinois 62901-4401*

(Received 27 June 1990; revised manuscript received 30 August 1991)

From the specific-heat (C_p) measurements on the isostructural $\text{NH}_4L(\text{SO}_4)_2 \cdot 4\text{H}_2\text{O}$ ($L = \text{La}, \text{Ce}, \text{Pr}, \text{Nd}, \text{Sm}, \text{Eu}, \text{Gd},$ and Tb) crystals at $100 \text{ K} < T < 300 \text{ K}$, it is shown that these crystals undergo two structural phase transitions, T_1 and T_2 , in the aforesaid temperature range. The observed shapes of the anomalies in the specific heat and their associated entropies are such that $\text{NH}_4\text{La}(\text{SO}_4)_2 \cdot 4\text{H}_2\text{O}$ crystals have a low-temperature phase-transition behavior that is different from that observed in $\text{NH}_4L(\text{SO}_4)_2 \cdot 4\text{H}_2\text{O}$ ($L = \text{Ce}, \text{Pr}, \text{Nd}, \text{Sm}, \text{Eu}, \text{Gd},$ and Tb). Also, our room-temperature infrared results and unit-cell parameters of $\text{NH}_4\text{Dy}(\text{SO}_4)_2 \cdot 4\text{H}_2\text{O}$ crystals indicate that the lattice is isostructural with the rest of the series but no transitions occur at $100 \text{ K} < T < 300 \text{ K}$. Unlike other isostructural lanthanide series, the phase-transition temperatures for $\text{NH}_4L(\text{SO}_4)_2 \cdot 4\text{H}_2\text{O}$ show no straightforward correlation either with the unit-cell parameters or with the host-lanthanide-ion's ionic radius. Further, the lattice-stability model, which successfully maps the trend of phase-transition temperatures for isostructural lanthanide orthoaluminates or pentaphosphates, is inadequate for predicting the observed behavior of $\text{NH}_4L(\text{SO}_4)_2 \cdot 4\text{H}_2\text{O}$ lattices.

I. INTRODUCTION

Trivalent lanthanides ($L = \text{La}, \text{Ce}, \text{Pr}, \text{Nd}, \text{Sm}, \text{Eu}, \text{Gd}, \text{Tb}, \text{Dy}, \text{Ho}, \text{Er}, \text{Tm}, \text{Yb},$ and Lu), because of their electronic configuration and size, form a number of isostructural insulating lattice series with various anions, e.g., $L(\text{OH})_3$, $L_2(\text{SO}_4)_3 \cdot 8\text{H}_2\text{O}$, $L\text{Cl}_3 \cdot 6\text{H}_2\text{O}$, $L(\text{C}_2\text{H}_5\text{SO}_4)_3 \cdot 9\text{H}_2\text{O}$, $L(\text{BrO}_3)_3 \cdot 9\text{H}_2\text{O}$, LP_5O_{14} , etc. This potential to form isostructural monocrystal series has led researchers to investigate these systems for host-lattice effects^{1,2} and for comparative magnetic interactions.²⁻⁴ In host-lattice effects, a particularly puzzling behavior is observed. For some isostructural series, the zero-field splitting of the doped S -state Gd^{3+} ions monotonically increases as the ionic radius of the host increases; while for other isostructural series, the zero-field splitting monotonically decreases as the ionic radius of the host increases. Equally puzzling behavior seems to be emerging for structural phase transitions in isostructural lanthanide lattices. As with the host-lattice effects, the structural-phase-transition temperature in $L_2(\text{MoO}_4)_3$ ($L = \text{Pr}, \text{Nd}, \text{Sm}, \text{Eu}, \text{Gd}, \text{Tb}, \text{Dy},$ and Ho) monotonically increases as the ionic radius of the host-lanthanide in-

creases.⁵ In LP_5O_{14} ($L = \text{La}, \text{Ce}, \text{Pr}, \text{Nd}, \text{Sm}, \text{Eu}, \text{Gd},$ and Tb), the structural-phase-transition temperature linearly decreases as the ionic radius of the host-lanthanide increases.⁶ More recently, Buchner *et al.*⁷ reported that the transition temperature in the superconducting $LBa_2Cu_3O_{7-y}$ ($L = \text{Nd}, \text{Eu}, \text{Gd}, \text{Dy}, \text{Ho}, \text{Er}, \text{Tm},$ and Yb) scales linearly with the lanthanide ionic radius. For the $LBa_2Cu_3O_{7-y}$, the graph of ionic radius versus the transition temperature exhibits a positive slope. Whether the aforesaid linear dependence between some physical property of the lattice (ionic radius of the lanthanide host or crystallographic parameters) and the transition temperature holds for other isostructural lattices is yet to be determined. Further, the physical mechanism(s) which can account for the sign of the slope need to be described.

Eriksson *et al.*⁸ reported that ammonium lanthanide sulfate tetrahydrate (ALSTH), $\text{NH}_4L(\text{SO}_4)_2 \cdot 4\text{H}_2\text{O}$, where $L = \text{La}, \text{Ce}, \text{Pr}, \text{Nd}, \text{Sm}, \text{Eu}, \text{Gd},$ and Tb , result in an isostructural monocrystal series. As can be expected, the ionic radius of lanthanide scales linearly with the cube root of the unit-cell volume for ALSTH. Malhotra *et al.*⁹ and Buckmaster *et al.*¹⁰ from their EPR mea-

measurements on $\text{NH}_4\text{L}_{0.99}\text{Gd}_{0.01}(\text{SO}_4)_2 \cdot 4\text{H}_2\text{O}$ ($L = \text{Ce}$ and Sm), suggest that these lattices undergo multiple structural phase transitions at $100 < T < 300$ K. Also, from EPR measurements at two temperatures (i.e., 77 and 298 K), Malhotra *et al.*¹¹ speculated that ANdSTH undergoes a structural transformation somewhere between 77 and 298 K. Since isostructural members of lanthanide series generally reflect similar thermodynamic properties, it will be reasonable to expect that ANdSTH also undergoes similar multiple phase transitions as those observed for ACeSTH and ASmSTH. However, it must be granted that it is not necessary for all the members of an isostructural series to display similar phase-transition behavior, as argued by Rousseau *et al.*¹²

In this paper we report our specific-heat results on ALSTH ($L = \text{La}$, Ce , Pr , Nd , Sm , Eu , Gd , Tb , and Dy), obtained with the help of a differential-scanning-calorimetry (DSC) technique. The measurements were undertaken with a view to ascertain (a) whether all the members of the ALSTH series display similar phase-transition behavior and (b) whether transition temperatures, especially since two members of the series display multiple transitions, show any dependence on the crystallographic parameters. It will be demonstrated from the specific-heat results that not all the members of the ALSTH series have similar thermodynamic properties at $100 < T < 310$ K. Also, it will be shown that crystallographic parameters do not, at least in a straightforward way, influence the structural phase transition temperatures for ALSTH.

II. EXPERIMENT

A. Crystal growth and infrared characterization

Eriksson *et al.*⁸ advocated that the monocrystals of ALSTH ($L = \text{La}$, Ce , Pr , Nd , Sm , Eu , Gd , and Tb) can be grown by slow evaporation of the aqueous solution containing 4:1 molar ratio of ammonium sulfate and lanthanide sulfate octahydrate. On the other hand, Il'yashenko *et al.*¹³ reported that, for $L = \text{Eu}$, Gd , and Tb , equimolar ratios of the component sulfates are sufficient to yield the lanthanide tetrahydrate double sulfate crystals. We attempted to grow monocrystals of ALSTH ($L = \text{La}$, Ce , Pr , Nd , Sm , Eu , Gd , Tb , Dy , Er , and Tm) using both 1:1 and 4:1 molar ratios. For 1:1 molar ratio, the results were erratic. Although for ACeSTH, APrSTH, and ANdSTH well-defined, prismatic crystals were produced, this was not the case for the rest of the lanthanide double-sulfate series. The crystals grown from 4:1 molar ratio of ammonium sulfate and lanthanide sulfate octahydrate generally produced prismatic ALSTH crystals. However, the use of excess $(\text{NH}_4)_2\text{SO}_4$ in the aqueous solution frequently results in the growth of both prismatic ALSTH crystals and $(\text{NH}_4)_2\text{SO}_4$ crystals. Before experimental measurements on ALSTH crystals can be made, they must be separated from the ammonium sulfate crystals. Since ammonium sulfate's solubility in water is much greater than ALSTH, the separation can be accomplished by washing the mixture with distilled water. Our attempts to grow AErSTH and ATmSTH monocrystals, irrespective of the amount of ammonium

sulfate and erbium sulfate or thulium sulfate used, were not successful.

The infrared (IR) spectra of the grown crystals were recorded with a view to ensure that the crystals under investigation were ALSTH monocrystals with $P2_1/c$ structure and not a mixture of lanthanide sulfate and ammonium sulfate. The IR spectra were acquired using the nujol and fluorolube mull techniques at room temperature on an IBM IR-32 Fourier-transform infrared spectrometer. The observed IR spectra of ALSTH ($L = \text{La}$, Ce , Pr , Nd , Sm , Eu , Gd , Tb , and Dy) grown with the 4:1 ratio are shown in Fig. 1 in the region $1350\text{--}4000$ cm^{-1} . Our IR analysis indicates that the water's bending modes at around 1640 cm^{-1} and ammonium ion's vibrations around at 1430 (ν_4), 2855 ($2\nu_4$), 3060 (ν_1), and 3270 (ν_3) could be used to determine when grown crystals of ALSTH deviate from their expected phase. Eriksson *et al.*⁸ reported that dysprosium forms a double sulfate with ammonium having composition of $\text{NH}_4\text{Dy}(\text{SO}_4)_2 \cdot 4\text{H}_2\text{O}$, but the resulting crystals have a structure different from ALSTH. However, a direct comparison of the vibrational spectrum of the Dy compound with the spectra of the other lanthanide double sulfates indicates that the ADySTH monocrystals, prepared in our laboratory, are isostructural with the other ALSTH. This was further checked by determining the unit-cell parameters of ADySTH. The unit cell was monoclinic with $a = 0.6512(2)$ nm, $b = 1.811(6)$ nm, $c = 0.8658(7)$ nm, and $\beta = 96.59(4)^\circ$. The unit-cell volume, i.e., $V = 105.36(9)$ $(\text{nm})^3$, fits in well with the monotonic decreases in $V^{1/3}$ when plotted against the ionic radius of the trivalent lanthanide as shown in Fig. 2. The graph in Fig. 2 can be represented by a simple linear relation $V^{1/3}$ (nm) = $0.843 + 1.614$ (ionic radius) with a regression-coefficient square = 0.999. This confirms the result, deduced from the vibrational investigation, that ADySTH,

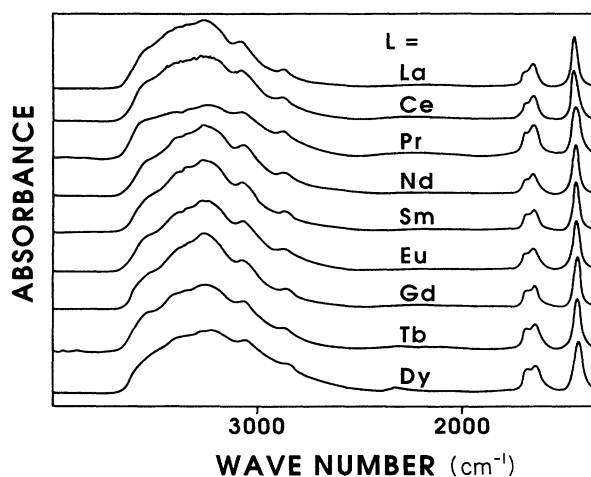


FIG. 1. Infrared spectra of isostructural $\text{NH}_4\text{L}(\text{SO}_4)_2 \cdot 4\text{H}_2\text{O}$ ($L = \text{La}$, Ce , Pr , Nd , Sm , Eu , Gd , Tb , and Dy) crystals showing the similarities between the ammonium and water structure for the series. These spectra were recorded with the help of a mull technique and, therefore, are only representative spectra not suitable for quantitative comparisons.

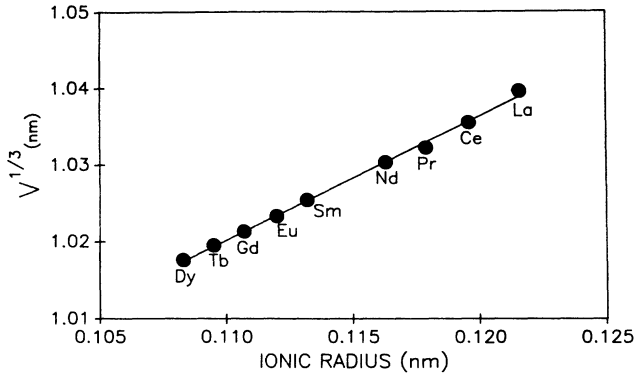


FIG. 2. Graph showing the variation of $V^{1/3}$ as a function of lanthanide-ions ionic radius for isostructural $\text{NH}_4\text{L}(\text{SO}_4)_2 \cdot 4\text{H}_2\text{O}$ series. The data points, except for Dy, are from Ref. 8.

not ATbSTH, is the last member of the isostructural $\text{NH}_4\text{L}(\text{SO}_4)_2 \cdot 4\text{H}_2\text{O}$ series.

B. Specific-heat measurements

Specific-heat measurements were made at $100 < T < 310$ K using the DSC technique. Single crystals of ALSTH were reduced in size by light hand grinding in an agate mortar to maximize the area of thermal contact between sample and pan. The microcrystals were hermetically sealed in Al pans by crimping them with Al lids. Sample masses of the order of 30 mg were high enough to give adequate sensitivity and low enough to avoid significant temperature gradients (thickness < 1 mm) within the samples. All sample masses were determined after encapsulation with an accuracy of ± 0.01 mg.

Calorimetric data for the specific-heat measurements were recorded on a Perkin-Elmer DSC7 system interfaced with a Perkin-Elmer 7700 computer. The calorimeter was calibrated for temperature and enthalpy, applying the procedure reported in the literature.^{14,15} The temperature calibration was performed by the two-point method, using the transitions¹⁶ in cyclohexane (obtained from NBS) at 186 K (solid-solid) and 280 K (melting). Within this bracketed range, the temperature calibration was checked against the ferroelectric transition¹⁷ of $(\text{NH}_4)_2\text{SO}_4$ at 224 K, and the error was found to be less than 0.5 K. Outside the bracketed range at the low-temperature end, the well-documented structural transitions¹⁷ in $\text{NH}_4\text{H}_2\text{PO}_4$ ($T_c = 148$ K) and KH_2PO_4 ($T_c = 123$ K) were used as calibration checks. The observed transition temperatures occurred reproducibly within $(T_c \pm 0.1)$ K for $\text{NH}_4\text{H}_2\text{PO}_4$ and $(T_c - 3)$ K for KH_2PO_4 . The dynamic temperature calibration, using the two-point method, was accomplished as outlined by ASTM standard practice.¹⁸ The slope and intercept of the assumed linear temperature scale of the calorimeter was calculated. The corrected transition temperatures were then obtained using the following equation:

$$T = (0.8929)T_{\text{observed}} + 15.86, \quad 120 < T < 150 \text{ K} . \quad (1)$$

The accuracy in temperature between 140 and 300 K, based on the above calibration procedure, was estimated to be ± 1 K. The enthalpy calibration was performed using indium heat of fusion as the standard. After the enthalpy calibration, the DSC data on cyclohexane was rerecorded; and the observed enthalpy of solid-solid transition and solid-liquid transition was consistent with those reported in the literature.¹⁹ The conditions under which the instrument calibration was performed exactly matched the experimental-run conditions, namely, scan rate, liquid- N_2 coolant, and He purge at 0.207-MPa pressure. Also, during both calibration and experimental runs, the dry-box assembly over the sample head was flushed with high-purity N_2 gas to prevent the condensation of moisture.

The specific-heat data on ALSTH was recorded using the experimental procedures outlined in Refs. 14 and 19–21. This involved scans on an empty sample pan, followed by scans on the same sample pan but with a sample in it. Heating rates of 20 and 40 K/min were used. Differences between the observed sample transition temperatures at the two scan rates were less than ± 1 K, which is the estimated uncertainty in temperature calibration. The data recorded at 40 K/min is presented here. The specific heat of a sapphire standard (Perkin-Elmer Part No. 0219-0136) was determined as a monitor to ascertain the accuracy of our equipment. In addition to sapphire, the accuracy of the specific-heat measurements were verified using polystyrene (NBS standard reference material 705). The results agreed with literature values^{22,23} to within 2% at $135 < T < 300$ K. At $T < 135$ K, the error in C_p was larger ($< 5\%$) due to the lack of a suitable enthalpy calibrate.²⁴ Nevertheless, the error was systematic, allowing us to ascertain the relative behavior of C_p for the ALSTH.

III. RESULTS AND DISCUSSION

A. Structural phase transition

The specific-heat results at $100 < T < 300$ K for ALaSTH and ADySTH are shown in Fig. 3, while the experimental specific-heat data for ALSTH ($L = \text{Ce}, \text{Pr}$,

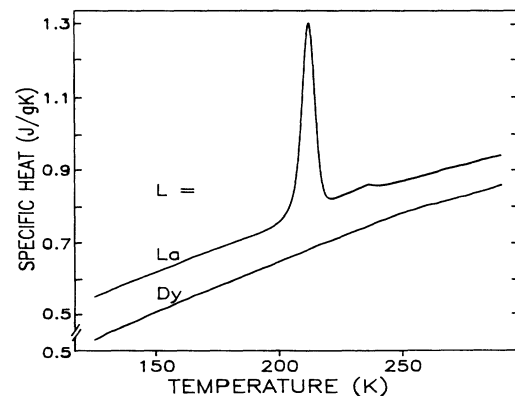


FIG. 3. The observed specific heat of $\text{NH}_4\text{L}(\text{SO}_4)_2 \cdot 4\text{H}_2\text{O}$ ($L = \text{La}$ and Dy) at $100 < T < 300$ K. The ordinate scale is the same for both curves.

tion was detected.

The EPR technique, sensitive to local influences, utilizes a dopant to study the host-lattice dynamics. It is possible that the additional phase transition, reported for ACeSTH and ASmSTH, may be an effect of doping. Recent reports^{25–27} on various doped systems have shown that doping at even very low concentrations can shift the transition temperature from that in the pure sample and may also cause a splitting of the transition. With the sparse experimental evidence that is currently available on the double-sulfate systems, it would be premature to draw any conclusions regarding this additional transition.

In order to determine the enthalpies associated with the phase transitions in ALSTH, the background specific heat is required. In an insulating system like ALSTH, the specific heat away from the anomalies is expected to be governed^{28,29} by

$$C(\text{background}) = (C_p - C_v) + C_l + C_i + C_r + C_e, \quad (2)$$

where $(C_p - C_v)$ is the dilation correction. C_l , C_i , and C_r are the contributions from the external lattice vibrations, the intramolecular vibrations from the polyatomic units (NH_4^+ , SO_4^{2-} and H_2O), and the rotational-librational motions of the ammonium ions and the water molecules, respectively. C_e is the contribution to the measured specific heat from any other source, e.g., lattice defects. The subtraction of $C(\text{background})$ from $C_p(\text{experimental})$ can be used quantitatively to understand the critical behavior of the transitions, provided there is sufficient experimental information to calculate $C(\text{background})$. Unfortunately, besides crystal structure⁸ and a few EPR (Refs. 9–11) measurements, no other data or studies are presently available on ALSTH, e.g., elastic constants and thermal-expansion coefficients required for the estimation of the dilation term, lattice modes for C_l , etc. In absence of the required data, ΔC_p [$=C_p(\text{experimental}) - C(\text{background})$] can be estimated by adopting one of two approaches. One is to fit the observed C_p to a polynomial in regions away from transitions as discussed in Refs. 21 and 30. The other is to use

$$\Delta C_p(\text{ALSTH}) = C_p(\text{ALSTH}) - C_p(\text{ADySTH}), \quad (3)$$

where $L = \text{La, Ce, Pr, Nd, Sm, Eu, Gd, and Tb}$. The adoption of Eq. (3) is justified since the superposition of the specific-heat curves of ADySTH and ALSTH (lattices

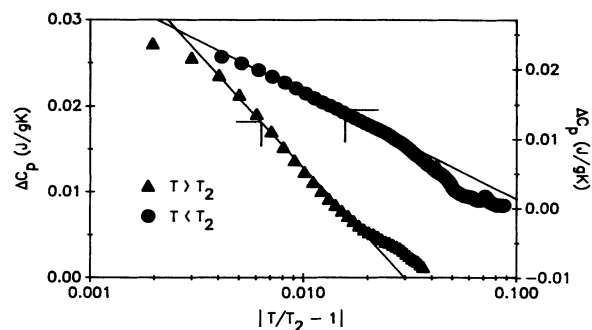


FIG. 5. The excess specific heat for the upper transition (T_2) of $\text{NH}_4\text{Pr}(\text{SO}_4)_2 \cdot 4\text{H}_2\text{O}$ vs the reduced temperature. The solid lines are the result of least-squares fits to a logarithmic singularity.

which undergo phase transitions) revealed similar temperature dependence in the regions away from the anomalies. Irrespective of the procedure adopted, i.e., polynomial fit or Eq. (3), the enthalpies and entropies calculated from the ΔC_p curves, listed in Table II, agreed within the given uncertainties. It can be noted from Table II that the entropies of the T_1 transitions tend to be larger for the ALSTH lattices having a Kramers' lanthanide ion (Ce, Nd, Sm, and Gd) than for those having a non-Kramers' ion (Pr and Tb) with the exception of the Eu lattice. The entropies associated with T_2 transitions showed no such trend. The significance of this observation, if any, is not clear to us at present.

The excess specific-heat curves (ΔC_p), obtained by using Eq. (3), revealed the T_2 anomaly had an asymmetric λ shape for the Ce, Pr, Nd, Sm, Eu, Gd, and Tb lattices. Since λ shapes are generally associated with order-disorder transitions,^{21,31} an attempt was made to fit ΔC_p to a logarithmic function

$$\Delta C_p = A \ln \epsilon + B, \quad (4)$$

where $\epsilon = |T/T_2 - 1|$. We also fitted the ΔC_p curves to a power law,

$$\Delta C_p = A' \epsilon^\alpha + B'. \quad (5)$$

Logarithmic behavior [Eq. (4)] in the critical regions, $\epsilon < 0.05$ for $T < T_2$ and $\epsilon < 0.02$ for $T > T_2$, was observed, as shown in Fig. 5, for APrSTH. The regression

TABLE II. Enthalpies (ΔH) and entropies (ΔS) of the structural phase transitions in isostructural $\text{NH}_4\text{L}(\text{SO}_4)_2 \cdot 4\text{H}_2\text{O}$ crystals.

System	Lower transition (T_1)			Upper transition (T_2)		
	T_1 (K)	ΔH (J/g)	ΔS (J/gK)	T_2 (K)	ΔH (J/g)	ΔS (J/gK)
La	212	3.6	0.017	236	0.10	0.0004
Ce	149	0.30	0.0020	254	0.22	0.0006
Pr	147	0.17	0.0011	263	0.22	0.0007
Nd	157	0.33	0.0021	269	0.33	0.0011
Sm	160	0.23	0.0014	273	0.29	0.0009
Eu	161	0.27	0.0016	273	0.38	0.0012
Gd	159	0.28	0.0015	269	0.4	0.0015
Tb	145	0.23	0.0011	266	0.27	0.0010

coefficients varied between 0.97 and 0.99. It is interesting to note that the specific heat could not be fitted by a power law [Eq. (5)] over reasonable ranges of ϵ . For a second-order Landau transition, a weak (logarithmic) singularity with specific-heat exponent $\alpha=0$ occurs.³² This confirms that the T_2 transition is of second order. However, the divergence in C_p is not as sharp as predicted, especially for $T > T_2$ (see Fig. 5). The rounding off is probably a consequence of the scanning technique employed rather than due to the intrinsic behavior of the materials at the transition.

B. Effects of lanthanide hosts

As seen from Table II, the transition temperature T_1 and its entropy for ALaSTH differ substantially from those in the intermediate ALSTH ($L = \text{Ce, Pr, Nd, Sm, Eu, Gd, and Tb}$). Also, from Figs. 3 and 4, a comparison of the shapes of the anomalies in specific heat shows that the nature of the T_1 transition in the La double sulfate is markedly different from that in the intermediate lanthanide double sulfates, while the T_2 transition is similar. For ADySTH, on the other hand, no phase transitions were observed at $100 < T < 300$ K even though our IR and unit-cell data suggested it to be isostructural with the rest of the ALSTH series. Based on the specific-heat results, the isostructural ALSTH ($L = \text{La, Ce, Pr, Nd, Sm, Eu, Gd, Tb, and Dy}$) can be divided into three groups: group I consists of the lone member of the series, i.e., ALaSTH; while group II consists of the intermediate members, i.e., ALSTH with $L = \text{Ce, Pr, Nd, Sm, Eu, Gd, and Tb}$; and group III again contains a single member of the isostructural series, i.e., ADySTH.

Typically the structural phase-transition temperature in an isostructural lanthanide series has shown a systematic trend with respect to the unit-cell parameters.^{5-7,33-38} To illustrate this, some of the data available for other lanthanide isostructural series have been listed in Table I, along with the results of the present study. We have graphed the dependence of the lower

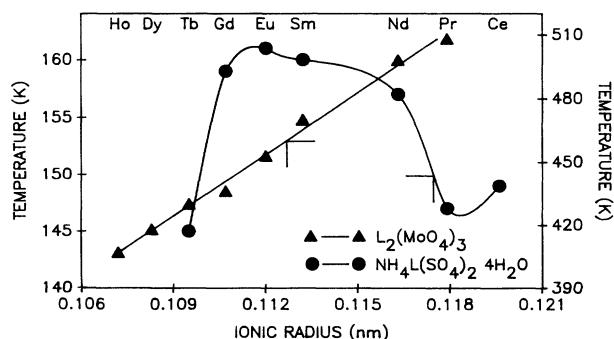


FIG. 6. This graph shows the dependence of the structural phase transition temperature on the lanthanide-ion ionic radius for isostructural $\text{NH}_4\text{L}(\text{SO}_4)_2 \cdot 4\text{H}_2\text{O}$ (lower transition, i.e., T_1) and for $\text{L}_2(\text{MoO}_4)_3$ series. The data for molybdates are from Ref. 5.

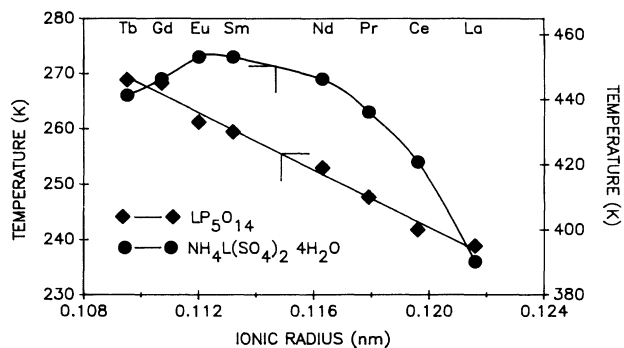


FIG. 7. Graph depicting the effect of the lanthanide host's ionic radius on the structural phase transition in isostructural $\text{NH}_4\text{L}(\text{SO}_4)_2 \cdot 4\text{H}_2\text{O}$ (upper transition, i.e., T_2) and in LP_5O_{14} series. The data for pentaphosphates are from Ref. 36.

phase transition temperature, i.e., T_1 , on the lanthanide ionic radius for group II of ALSTH in Fig. 6. Figure 7 depicts similarly graphed data of groups I and II for the upper transition temperature, i.e., T_2 . As can be seen from Figs. 6 and 7, no straightforward relationship exists between the lanthanide's ionic radius and T_1 or T_2 . This result is in contrast to other lanthanide series where the transition temperature (T_c) varies systematically with the ionic radius of the lanthanide ion (see Table I). For some series, e.g., the molybdates,⁵ the dependence is monotonic and positive. As the ionic radius decreases, T_c decreases. For other series, e.g., the pentaphosphates,⁶ the dependence is monotonic and negative. The decrease in ionic radius is accompanied by an increase in T_c ; for the lanthanide-substituted tungstates,³⁸ T_c first increases and then decreases with decreasing ionic radius.

An explanation for such trends has been sought in terms of the effect of the ionic size on the stability of the crystal structure above and below the transition temperature.^{5,6,33,34} If a large-radius L^{3+} ion is more effective in stabilizing the $T > T_c$ lattice, then the transition temperature will be lowered. The smaller L^{3+} ions will require a higher temperature to have the same effective radius, i.e., r_0 plus the thermal rms displacement due to phonons. Hence, the transitions in the corresponding lattices will occur at higher temperatures, and a negative, monotonic dependence of transition temperature on ionic radius will be observed. Conversely, if the $T < T_c$ lattice is stabilized by a larger L^{3+} ion, the transition temperature will be raised, and a positive, monotonic dependence will be expected. The lattice parameters across a lanthanide series, below or above the transition temperature, will provide an indicator of the distortion at the atomic level. The trend in distortion can then be directly correlated to the stability of the structure with respect to L^{3+} ionic size.

Applying the above-discussed lattice stability model to the molybdates, Brixner *et al.*⁵ considered the shear angle, θ , defined in terms of the orthorhombic splitting, $(b-a)$, to be the distortion parameter; while for the pentaphosphates, the deviation from orthorhombicity ($\delta = \beta - 90^\circ$) was taken by Weber *et al.*⁶ to be the operative parameter. The observed trends in the distortions, θ

and δ , with respect to the L^{3+} ionic radius are opposite, consistent with the opposite slopes observed for the transition temperature versus ionic radius plots for the respective isostructural series shown in Figs. 6 and 7.

In order to extend this heuristic model to the ALSTH series, we note that lattice parameters only at room temperature, i.e., $T > T_2$, have been determined.⁸ The monoclinic angle, β , is largest for ALSTH and decreases as the L^{3+} ionic radius decreases. This suggests that, for $T > T_2$, the ALSTH lattice is stabilized by a larger L^{3+} ion. Hence, a positive slope in the dependence of T_2 on ionic radius is expected. Figure 7 shows this to be true for only part of the series, up to ASmSTH. For smaller L^{3+} lattices, the trend is reversed, suggesting that factors other than the size of the L^{3+} ion need to be considered to explain the observed behavior. For the lanthanide-substituted tungstate series, too, a reversal in transition temperature trend was reported³⁸ (see Table I) but found to be a consequence of a similar trend in unit-cell constants. For ALSTH, the unit-cell parameters vary monotonically with L^{3+} ionic radius so that the argument that applies to the tungstate series is not valid here. Our attempts to relate T_2 or T_1 with the room-temperature unit-cell parameters or the monoclinic distortion ($\text{ac}[\cos(\beta-90^\circ)]$) of ALSTH produced no meaningful trends.

The exact mechanism or mechanisms which drive the structural phase transitions in $\text{NH}_4L(\text{SO}_4)_2 \cdot 4\text{H}_2\text{O}$ will require additional measurements on these isostructural lattices, especially crystallographic and NMR measurements at $100 < T < 300$ K. We hope this report will stimulate such measurements since these isostructural systems can serve as excellent hosts to test various thermodynamic theories.

IV. SUMMARY AND CONCLUSIONS

Based on the room-temperature infrared and temperature-dependent specific-heat measurements on isostructural $\text{NH}_4L(\text{SO}_4)_2 \cdot 4\text{H}_2\text{O}$ ($L = \text{La, Ce, Pr, Nd, Sm, Eu, Gd, Tb, and Dy}$) lattices at $100 < T < 300$ K, we conclude the following: (1) The infrared spectrum and the unit-cell parameters of $\text{NH}_4\text{Dy}(\text{SO}_4)_2 \cdot 4\text{H}_2\text{O}$ lattice reveal that Dy is the last isostructural member of the series, not Tb as suggested in the literature. (2) The specific-heat results have shown that all the members of the $\text{NH}_4L(\text{SO}_4)_2 \cdot 4\text{H}_2\text{O}$ series, except Dy, display two structural phase transitions at $100 < T < 300$ K. However, the behavior of the low-temperature transition in the La lattice is different from that in the rest of the series even though all the lattices are isostructural. (3) Contrary to the observed behavior of phase-transition temperature in isostructural lanthanides series reported in the literature, the transition temperatures in $\text{NH}_4L(\text{SO}_4)_2 \cdot 4\text{H}_2\text{O}$ show no straightforward relationship either with the unit-cell parameters or with the ionic radius of the host lanthanide ion. The lattice stability model, which can explain the trend of transition temperatures in isostructural lanthanide orthoaluminates or pentaphosphates, is inadequate to explain the observed trend of phase-transition temperatures in $\text{NH}_4L(\text{SO}_4)_2 \cdot 4\text{H}_2\text{O}$.

ACKNOWLEDGMENTS

The authors express their appreciation to P. D. Robinson of the Department of Geology for providing the x-ray facilities for the unit-cell parameter determination and Professor N. Ali of the Department of Physics for running the magnetic-susceptibility scans.

¹V. M. Malhotra, H. D. Bist, and G. C. Upreti, *J. Chem. Phys.* **69**, 1919 (1978).

²V. M. Malhotra and H. A. Buckmaster, *Can. J. Phys.* **60**, 1573 (1982).

³F. Mehran and K. W. H. Stevens, *Phys. Rev. B* **27**, 2899 (1983).

⁴V. M. Malhotra, H. A. Buckmaster, and K. A. Kerr, *J. Chem. Phys.* **82**, 2880 (1985).

⁵L. H. Brixner, P. E. Bierstedt, A. W. Sleight, and M. S. Licis, *Mater. Res. Bull.* **6**, 545 (1971).

⁶H. P. Weber, B. C. Tofield, and P. F. Liao, *Phys. Rev. B* **11**, 1152 (1975).

⁷B. Buchner, U. Callieb, H. D. Jostarndt, W. Schlabitz, and D. Wohlleben, *Solid State Commun.* **73**, 357 (1990).

⁸B. Eriksson, L. O. Larsson, L. Niinisto, and U. Skoglund, *Inorg. Chem.* **13**, 290 (1974).

⁹V. M. Malhotra, H. A. Buckmaster, and H. D. Bist, *Can. J. Phys.* **58**, 1667 (1981).

¹⁰H. A. Buckmaster, V. M. Malhotra, and H. D. Bist, *Can. J. Phys.* **59**, 596 (1981).

¹¹V. M. Malhotra, H. D. Bist, and G. C. Upreti, *Chem. Phys. Lett.* **28**, 390 (1974).

¹²J. Rousseau, J. Y. Gresland, J. Julliard, J. Nouet, J. Zarembowitch, and A. Zarembowitch, *Phys. Rev. B* **12**, 1279 (1975).

¹³V. S. Il'yashenko, A. I. Barabash, V. I. Volk, L. L. Zaitseva,

M. I. Konarev, A. A. Kruglov, and L. V. Lipis, *Zh. Neorg. Khim.* **14**, 1197 (1969) [*Russ. J. Inorg. Chem.* **14**, 627 (1969)].

¹⁴S. C. Mraw, *Specific Heat of Solids*, edited by C. Y. Ho (CINDAS Data Series on Material Properties, Purdue University, Lafayette, IN, 1988), Vol. I-2, Chap. 11.

¹⁵J. E. Callanan and S. A. Sullivan, *Rev. Sci. Instrum.* **57**, 2584 (1986).

¹⁶J. G. Aston, G. J. Szasz, and H. L. Fink, *J. Am. Chem. Soc.* **65**, 1135 (1943).

¹⁷M. E. Lines and A. M. Glass, *Principles and Applications of Ferroelectrics and Related Materials* (Clarendon, Oxford, 1977).

¹⁸*Standard Practice E967-83, Annual Book of Standards* (American Society for Testing and Materials, Philadelphia, 1988), Vol. 14-02, p. 583.

¹⁹S. C. Mraw and D. F. Naas-O'Rourke, *J. Chem. Thermodyn.* **12**, 691 (1980).

²⁰W. Wendlandt, *Thermal Analysis* (Wiley, New York, 1986).

²¹H. J. Fecht, Z. Fu, and W. L. Johnson, *Phys. Rev. Lett.* **64**, 1753 (1990).

²²D. C. Ginnings and G. T. Furukawa, *J. Am. Chem. Soc.* **75**, 522 (1953).

²³D. McIntyre and S. S. Chang, National Bureau of Standards

- Certificate, Standards Reference Material 705 (U.S. GPO, Washington, D.C., 1978).
- ²⁴J. E. Callanan, K. M. McDermott, and E. F. Westrum, Jr., *J. Chem. Thermodyn.* **22**, 225 (1990).
- ²⁵U. J. Cox, A. Gibaud, and R. A. Cowley, *Phys. Rev. Lett.* **61**, 982 (1988).
- ²⁶R. S. Rubins, J. E. Drumheller, and S. L. Hutton, *J. Chem. Phys.* **91**, 3614 (1989).
- ²⁷H. W. den Hartog and J. van der Veen, *Phys. Rev. B* **37**, 1807 (1988).
- ²⁸R. J. C. Brown, R. D. Weir, and E. F. Westrum, Jr., *J. Chem. Phys.* **91**, 399 (1989).
- ²⁹R. J. C. Brown, J. E. Callanan, R. D. Weir, and E. F. Westrum, Jr., *J. Chem. Phys.* **85**, 5963 (1986).
- ³⁰R. S. Kwok, G. Gruner, and S. E. Brown, *Phys. Rev. Lett.* **65**, 365 (1990); B. Cort and D. G. Naugle, *Phys. Rev. B* **24**, 3884 (1981); A. Migliori, W. M. Visscher, S. E. Brown, Z. Fisk, S. W. Cheong, B. Alten, E. T. Ahrens, K. A. Kubat-Martin, J. D. Maynard, Y. Huang, D. R. Kirk, K. A. Gillis, H. K. Kim, and M. H. W. Chan, *ibid.* **41**, 2098 (1990).
- ³¹K. M. Cheung and F. G. Ullman, *Phys. Rev. B* **10**, 4760 (1974).
- ³²E. Salje and B. Wruck, *Phys. Rev. B* **28**, 6510 (1983).
- ³³J. F. Scott, *Rev. Mod. Phys.* **46**, 83 (1974).
- ³⁴J. F. Scott and J. P. Remeika, *Phys. Rev. B* **1**, 4182 (1970).
- ³⁵C. P. Poole, Jr., H. A. Farach, and R. J. Creswick, *Ferroelectrics* **71**, 143 (1987).
- ³⁶C. Ting and H. Guang-Yen, *Acta Phys. Sin. (Jpn.)* **35**, 1521 (1986).
- ³⁷M. L. Vrtis, J. D. Jorgensen, and D. G. Hinks, *J. Solid State Chem.* **84**, 93 (1990).
- ³⁸L. I. Shvorneva and Yu. N. Venevtsev, *Bull. Acad. Sci. USSR Phys. Ser.* **33**, 1071 (1969).